

Catadioptric Camera Calibration

Christopher Geyer and Kostas Daniilidis
GRASP Laboratory, Computer and Information Science Department
University of Pennsylvania, {cgeyer,kostas}@grip.cis.upenn.edu*

Proceedings International Conference on Computer Vision 1999, pp. 398-404

Abstract

Catadioptric systems are realizations of omnidirectional vision through mirror-lens combinations. Designs preserving the uniqueness of an effective viewpoint have recently gained attraction. We present here a novel approach for estimating the intrinsic parameters of a well-known catadioptric system consisting of a paraboloid mirror and an orthographic lens. We introduce the geometry of catadioptric line projection and we show that the vanishing points lie on a conic section which encodes the entire calibration information. Projections of two sets of parallel lines suffice for intrinsic calibration from one view as well as for metric rectification of a plane. Our approach overcomes limitations of existing manual calibration methods and was successfully tested on the task of back-warping real-images images onto virtual planes.

1. Introduction

It is common sense in computer vision that increasing the field of view enhances several visual capabilities like ego-motion estimation and localization [8, 3]. It has been further proved that uncertainty in ego-motion estimates depends on the shape of the imaging surface (planar or spherical); in the spherical case it is lower than in the case of planar imaging surfaces [4]. The advantages of omnidirectional sensing are obvious for applications like surveillance, immersive telepresence, videoconferencing, mosaicing, and map building. A panoramic field of view eliminates the need for more cameras or a mechanically turnable camera.

A panoramic field of view camera was first proposed by Rees [12]. After 20 years the concept of omnidirectional sensing was reintroduced in robotics [16]

for the purpose of autonomous vehicle navigation. In the last five years, several omnidirectional cameras have been designed for a variety of purposes. The rapid growth of multimedia applications has been a fruitful testbed for panoramic sensors [9, 10, 11] applied for visualization. Another application is telepresence [13, 1] where the panoramic sensor achieves the same performance as a remotely controlled rotating camera with the additional advantage of an omnidirectional alert awareness. Srinivasan [2] designed omnidirectional mirrors that preserve ratios of elevations of objects in the scene and Hicks [7] constructed a mirror-system that rectifies planes perpendicular to the optical axis. The application of mirror-lens systems in stereo and structure from motion has been prototypically described in [14, 6].

Omnidirectional sensing can be realized with dioptric or catadioptric systems. Dioptric systems consist of fish-eye lenses while catadioptric systems are combinations of mirrors and lenses. These sensors can be separated into two classifications, determined by whether they have a unique effective viewpoint. Conical and spherical mirror systems as well as most fish-eye lenses do not possess a single vantage-point. Among those that do have a unique effective viewpoint are systems which are composed of multiple planar mirrors and perspective cameras all of whose viewpoints coincide, as well as a hyperbolic mirror in front of a perspective camera, and a parabolic mirror in front of an orthographic camera [9]. The uniqueness of a projection point is equivalent to a purely rotating planar camera with the nice property that a rotated image is a collineation of an original one. Hence, every part of an image arising from such a catadioptric sensor can easily be rewarped into the equivalent image of a planar camera looking to the desired direction without knowledge of the depths of the scene.

The distortion removal presumes an exact alignment of the mirror and the lens as well as the knowl-

*This work has been supported by ARO/MURI DAAH04-96-1-0007, NSF GER93-55018, and NSF CDS-97-03220.

edge of the optical parameters of both. In this paper we present the theory and an algorithm for the intrinsic calibration of a commercially available catadioptric system comprising a parabolic mirror and an orthographic lens [10]. The only method for intrinsic calibration of this system has been manual with the requirement that the parabolic mirror is entirely visible in the image. The user must determine by eye the projection of its center as well as the radius of the projection.

In this paper we propose a new approach for the recovery of the intrinsic parameters of a parabolic catadioptric system. Our approach is applicable even if only a part of the mirror is visible in the image and does not require manual interaction or human estimation. The only requisite is the detection of two sets of parallel lines in the scene.

We develop a theory that describes the projection of parallel lines on such a catadioptric system. Given that the pixel aspect ratio is equal to one, parallel lines project onto circular arcs whose centers are collinear. When the aspect ratio is not one we obtain elliptical arcs instead of circular arcs; the ratio of coefficients of the ellipse directly reveal the aspect ratio. The projection mapping of a parabolic-orthographic system preserves incidence relationships. Therefore, the vanishing point of a set of parallel lines projects onto the intersection of the circular arcs with the property that we obtain two vanishing points for each set, one in each direction. We will prove that

1. The image center is equal to the intersection of the lines connecting the vanishing points.

2. The vanishing points that originally lie on a line in the plane at infinity (horizon) are projected to a circle. The distance of this horizon circle to the image center reveals the unknown scaling factor which is the product of the lens and the mirror focal lengths.

3. The normal of the two sets of parallel lines can be directly estimated from the center of the horizon circle.

It should be noted that planar projection cameras can also be calibrated using vanishing points. It is already textbook material [15] that the three vanishing points arising from the perspective projection of a cube determine the image center, i.e. the orthocenter of the triangle of the three vanishing points. However, this is possible only if the aspect ratio is equal to one. In our approach we use only two sets of parallel lines and do not assume orthogonality of lines. No intrinsic calibration is possible with such minimal data in the case of a planar lens-camera. Our approach resembles the recovery of intrinsics from a purely rotating planar camera. The approach can be easily adapted to cali-

brating hyperbolic mirrors with perspective lenses.

2. Geometric Properties of a Parabolic Mirror

The simplest rotationally symmetric paraboloid is described by the implicit equation

$$z = \frac{1}{4f}(x^2 + y^2).$$

The parameter f determines the distance from the vertex of the paraboloid, located at the origin, to the focal point which lies on the optical axis Fig. 1). The optical axis in this case is the z -axis. The special property of the parabolic mirror which makes it so useful is that any ray of light which is parallel to the optical axis of the mirror will be reflected so that the reflected ray appears as though it originated from this focal point. We use the inverse property, that is, the reflection of a ray which intersects the focal point will be a ray which is parallel to the optical axis. It is assumed that the op-

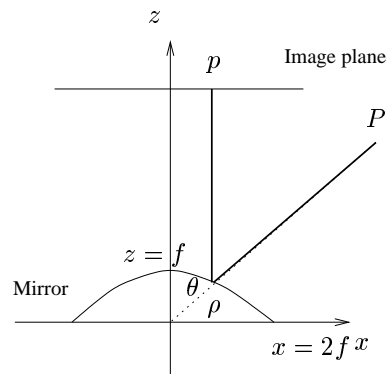


Figure 1: An xz -section of the catadioptric system.

tical axis of the parabolic mirror is perpendicular to the imaging surface. The projection of the particular lens we use can be approximated by an orthographic projection to a sufficient enough degree that it is indistinguishable from one. In addition we shift the origin of our coordinate system to the focal point and set the positive z -semi-axis in the visible space so that the equation of the paraboloid reads

$$z = f - \frac{1}{4f}(x^2 + y^2). \quad (1)$$

The mapping to pixel coordinates (x_p, y_p) in the image involves a shift and a scaling:

$$x_p = s_x x + x_0 \quad y_p = s_y y + y_0 \quad (2)$$

The two scale factors s_x and s_y depend on the focal length of the lens, the cell-size of the CCD-chip, and

the sampling rate of the frame-grabber. When a point (x, y, z) in space is projected to the image point (x_p, y_p) the focal length of the mirror can not be distinguished from the scaling factors of the camera.

The task of intrinsic calibration is to compute the two scaling factors and the image center. We will first work in the so called normalized image coordinate system (x, y) where the image center is at $(0, 0)$ and the common scaling factor is the focal length of the paraboloid. Given a point p_i in space, its image p'_i is the orthographic projection of the intersection of the line containing p_i and the focal point.

Given a line ℓ_i with direction $\hat{\ell}_i$ and containing the point p_1 , denote the normal of the plane P_i containing both ℓ_i and the focal point (the origin) by \hat{n}_i . The normal is chosen w.l.o.g. to have a positive z-component. If ℓ_i does intersect the focal point we will not consider it a valid line since its image will be a point. The orthographic projection of the intersection of the plane P with the surface of the mirror, is the image ℓ'_i of the line ℓ_i .

Proposition 1 *The image of a line is a circular arc if the line is not parallel to the optical axis. A line is projected onto a line if it is parallel to the optical axis.*

Proof: The normal corresponding to a line parallel to the optical axis is $\hat{n} = (n_x, n_y, 0)$. Since this implies that the plane is perpendicular to the image plane, the orthographic projection of its intersection with the paraboloid will be a line with equation $n_x x + n_y y = 0$.

When the line is not parallel to the optical axis the normal reads $\hat{n} = (n_x, n_y, n_z)$ with $n_z \neq 0$. The plane can be written as

$$z = -\frac{n_x}{n_z}x - \frac{n_y}{n_z}y = Ax + By.$$

To obtain the intersection of the plane with the paraboloid we insert z into (1)

$$\begin{aligned} Ax + By - f + \frac{1}{4f}(x^2 + y^2) &= 0 \\ -4f^2 + x^2 + y^2 + 4fAx + 4fBy &= 0. \end{aligned}$$

This is the implicit equation of a circle with center (c_x, c_y) and radius r given by

$$\begin{aligned} c_x &= -2fA = 2f\frac{n_x}{n_z}, \\ c_y &= -2fB = 2f\frac{n_y}{n_z}, \\ r &= \frac{2f}{n_z}\sqrt{n_x^2 + n_y^2 + n_z^2} = \frac{2f}{n_z}. \end{aligned}$$

When the image ℓ'_i is the arc of a circle denote the circle containing it by α_i with radius α_i^r and center (α_i^x, α_i^y) . When ℓ'_i is a line indicate this by calling it β_i .

Proposition 2 *The intersection of two circles which are projections of parallel lines depends only on the common direction and not on the positions of the parallel lines. The image center lies in the line segment connecting the two intersection points.*

Proof: Two parallel lines in space define two planes with normals \hat{n}_1 and \hat{n}_2 when connected to the origin unless both lines and the origin lie on the same plane. In this case the images of the lines are identical and we cannot speak of an intersection.

In the general case, the intersection of the two planes is a line with direction $\hat{n}_1 \times \hat{n}_2$. If the common direction of the parallel lines is \hat{l} then both \hat{n}_1 and \hat{n}_2 are perpendicular to \hat{l} . Hence, $\hat{n}_1 \times \hat{n}_2$ is parallel to \hat{l} and the intersection depends only on the common direction. Since both planes contain the origin by definition the origin belongs to the intersection and lies between the two intersection points with the paraboloid. The parametric equation of the intersection line is $(x, y, z) = \lambda\hat{l}$ which inserted into (1) and solved for λ gives the two 3D-points on the hyperboloid. The intersection of the circles in the image is just the orthographic projection of these points which read in normalized coordinates:

$$\begin{aligned} p_1 &= \left(-\frac{2fl_x(1+l_z)}{l_x^2+l_y^2}, -\frac{2fl_x(1+l_z)}{l_x^2+l_y^2} \right), \\ p_2 &= \left(\frac{2fl_x(1-l_z)}{l_x^2+l_y^2}, \frac{2fl_x(1-l_z)}{l_x^2+l_y^2} \right). \end{aligned}$$

where $\hat{l} = (l_x, l_y, l_z)$ is the common direction of the lines with $\|\hat{l}\| = 1$.

As described above, we can also easily verify in the formulae that the points p_1 and p_2 are on opposite sides of the image center, so the line segment $\overline{p_1 p_2}$ does contain the image center. The points p_1 and p_2 are well known in the case of planar cameras as vanishing points.

Corollary 1 *Given a set of parallel lines ℓ_i , the centers of the circles α_i lie on the perpendicular bisector of $\overline{p_1 p_2}$ and hence they are collinear.*

Corollary 2 *The image center may be determined from the intersection of two line segments $\overline{p_{11} p_{21}}$ and $\overline{p_{12} p_{22}}$ arising from two sets of parallel lines with directions l_1 and l_2 , respectively.*

This means that we may determine the image center from only two sets of parallel lines! Thus, we have decoupled the estimation of the image center from the computation of the scaling factor.

Proposition 3 *The vanishing points of lines with coplanar directions lie on a circle.*

Proof: Suppose that all the line directions l_i are perpendicular to a common normal \hat{m} . This normal defines a plane through the focal point $m_x x + m_y y + m_z z = 0$. This plane does not necessarily contain any of the lines but it contains the intersections of the directional lines $\lambda \hat{l}_i$ with the paraboloid. We can argue similarly to proposition (1) that the projection of the intersection of this plane with the paraboloid on the image plane is a circle. It is claimed that the center and radius of the circle is

$$(c_x, c_y) = \left(\frac{2fm_x}{m_z}, \frac{2fm_y}{m_z} \right), \quad r = \frac{2f}{m_z}. \quad (3)$$

Choose \hat{l}_i to be the direction of one of the parallel line sets with $\hat{l}_i \cdot \hat{m} = 0$. With that constraint and after a considerable amount of algebra we find that the distance ρ from the vanishing point p_{1i} to (c_x, c_y) is

$$\rho^2 = \left(\frac{2fl_{xi}}{l_{zi}} + \frac{2fn_x(1+nz)}{nx^2+ny^2} \right)^2 + \left(\frac{2fl_{yi}}{l_{zi}} + \frac{2fn_y(1+nz)}{nx^2+ny^2} \right)^2 = \frac{4f^2}{n_z^2}.$$

This distance is independent of the line direction \hat{l}_i , hence the vanishing points lie on a circle.

Corollary 3 *The normal (or pan and tilt) of a plane in space can be estimated from two sets of parallel lines with directions parallel to this plane. The normal is independent of the focal length f but depends on the image center.*

Proposition 4 *The focal length, f , can be determined from the radius and center of a circle determined with the conditions described in Proposition 3.*

Proof: Let $a = r - d$ and $b = r + d$ where r is the radius of the circle in Proposition 3, and d is the distance from the image center to the circle's center. Then a is the least distance from a point on the circle to the image center, and b is the greatest distance from a point on the circle to the image center. The points which give the greatest and least distance from the image center are collinear with the image center, and are on opposite sides of the image center. Therefore the points $(-a, y_1)$ and (b, y_2) must satisfy

$$y = mx, \quad \text{and} \quad y = \frac{1}{4f}x^2.$$

Setting them equal and solving for m and f yields

$$m = \frac{b-a}{2\sqrt{b}}, \quad f = \frac{1}{2}\sqrt{ab}. \quad (4)$$

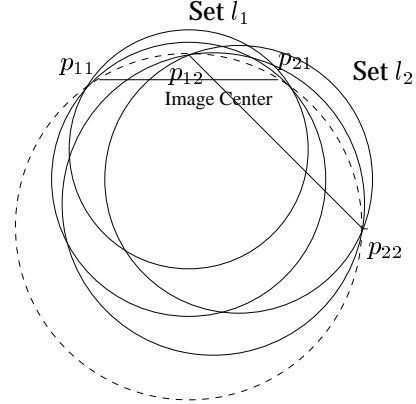


Figure 2: Two sets of circles arising from two sets of parallel lines with directions l_1 and l_2 , respectively. The circles arising from lines l_i intersect at vanishing points p_{1i} and p_{2i} . The locus of vanishing points is a circle (dashed-line).

3. Fitting Geometric Structures

In this section we describe the methods we used for fitting conics and obtaining intersection points in the presence of noise.

3.1. Fitting Circles

In the next section we will need to be able to fit a number of points in the image to a circle. We need to determine the parameters of the implicit equation

$$x^2 + y^2 + Cx + Dy + E = 0$$

from which we may obtain the center and radius,

$$(c_x, c_y) = (-C/2, -D/2),$$

$$r = \frac{1}{2}\sqrt{C^2 + D^2 - 4E}.$$

Given points $\{(x_i, y_i)\}_{i=1}^n$ we try to minimize the sum

$$E(C, D, E) = \sum_{i=1}^n (x_i^2 + y_i^2 + Cx_i + Dy_i + E)^2$$

by solving the system of equations

$$\frac{\partial E}{\partial C} = 0, \quad \frac{\partial E}{\partial D} = 0, \quad \text{and} \quad \frac{\partial E}{\partial E} = 0.$$

3.2. Determining Circle Intersection

We showed that the intersection of the image circles of parallel lines intersect at two points, and that the image circles' centers are collinear. The two intersection points correspond to the vanishing points and allow us to determine the image center. We would like to determine these two points in the presence of noise.

One way to do this would be to minimize a sum of the implicit equations over x and y using gradient descent. But this method is nonlinear and does not utilize the information in the constraint that the circles' centers are collinear. A better approach is to note that the radius of the circles as a function of distance along the line on which their centers lie, is a hyperbola. This is because the radius of the circle at some point on the line is equal to the distance to the two intersection points of all the circles. The intersections of all the circles are the vertices of the hyperbola described by $r^2 = a^2 - (x - b)^2$.

Given pairs of position and radius, $\{x_i, r_i\}$, we minimize the sum

$$\sum (r_i^2 - a^2 + (x_i - b)^2)^2$$

by taking its derivative with respect to a and b . Then set the two derivatives to 0 and solve for a and b . The parameter b gives the translation along the line, and a is the perpendicular distance from the line to the two intersection points (vertices).

4. Calibration Algorithm

Due to space limitations we describe here only the case of aspect ratio $s_x/s_y = 1$. If $s_x \neq s_y$, then we fit elliptical arcs instead of circular and rewrap the image using the ratio of the ellipse half-axes.

1. Obtain a set of points in the image which are the images of points on lines, such that the directions of all the lines are coplanar, and so that for every line there is another which is parallel to it.
2. To each set of points on a line, fit a circle as described in the previous section on fitting circles. Extract the radii and centers from the implicit equations of the fitted circles. Group the circles so that the lines, of which they are an image, are parallel (and thus the circles' centers are collinear). For example for some i the set of circles $\{\alpha_{i,j}\}_{j=1}^{n_i}$ are images of a set of parallel lines.
3. For each set of center collinear circles (parallel lines) $\{\alpha_{i,j}\}_{j=1}^{n_i}$, fit a line γ_i to their centers. Project the centers onto this line and determine their position on a unit linear parameterization of

the line. In other words for each projected center $(c_x^{j'}, c_y^{j'})$ determine t_i such that $\gamma(t_i) = (c_x^{j'}, c_y^{j'})$ where $\gamma_i(t)$ is the fitted line. Fit a hyperbola of the form

$$y = \sqrt{a_i^2 + (x - b_i)^2}$$

to the pairs (t_j, r_j) over the parameters a_i and b_i . Let \hat{n}_i be the normal of the fitted line (e.g. if $\gamma_i'(t) = (u, v)$ then $\hat{n}_i = (-v, u)$). The intersection of the collinear circles are two points

$$\begin{aligned} \pi_0^i &= \gamma_i(b_i) + a_i \hat{n}_i, \\ \pi_1^i &= \gamma_i(b_i) - a_i \hat{n}_i. \end{aligned}$$

4. Determine the intersection of the line segments $\overline{\pi_0^i \pi_1^i}$. Let $a_i x + b_i y = c$ be the implicit equation of the line containing the line segment $\overline{\pi_0^i \pi_1^i}$. We use the pseudoinverse (Moore-Penrose inverse) of the matrix

$$\begin{bmatrix} a_1 & b_1 \\ \vdots & \vdots \\ a_n & b_n \end{bmatrix}$$

multiplying it by the vector (c_1, \dots, c_n) to obtain the intersection point. This intersection is the image center, (c_x, c_y) .

5. Fit a circle to the points $\pi_{0,1}^i$. Let r be the radius of the circle, let c_0 be the center of the circle, and let d be the distance from the image center to c_0 . Then

$$f = \frac{1}{2} \sqrt{(r+d)(r-d)}.$$

5. Experiments

We present here two experiments with real images. We used the commercial S1 design of the catadioptric camera (Cyclovision, Inc.) invented by Nayar [10]. Our algorithm presumes the detection of edge elements or blob points and their grouping into clusters corresponding to elliptical arcs. This is accomplished by a Hough-transform in the four-dimensional space of ellipse parameters. After establishing a rough estimate of the parameters through the accumulator maxima we refit the elliptical arcs using the algorithm [5] described above.

After eliminating the aspect ratio we follow the steps of 5.1 starting by fitting circles. At the end we obtain the intrinsic parameters as well as the normal of the plane. In order to verify the accuracy of our estimates we backwarp the images by perspective projecting first onto a plane perpendicular to the optical axis. Assume that a point on the paraboloid is given by spherical coordinates (ρ, θ, ϕ) where (ρ, θ) as

shown in Fig. 1 and ϕ the azimuth angle. Using the intrinsic parameters we obtain the polar and azimuth angle from the pixel coordinates (x_p, y_p) . The perspective projection on the virtual plane perpendicular to the optical axis reads then $x_v = c \tan \theta \cos \phi$ $y_v = c \tan \theta \sin \phi$ where c a scaling factor tuning the size of the resulting image in pixels. The normal of the scene plane can be estimated from the center and the radius of the circle through the vanishing points using eq. (3). Using the direction of the normal we are able to rotate the virtual plane to a plane which is parallel to the scene plane since a pure rotation is just a collineation. The perpendicularity of edges on these planes gives the accuracy of the pan-tilt estimate.

In the first experiment we recorded a series of images of a dotted plane taken from several angles. We show in Fig. 3 the fitted circles to the two sets of parallel lines (middle) and the back-warping onto the virtual plane parallel to the scene plane. Although the geometric accuracy of the result is superior the visual appearance may be less impressive because we did not apply any sophisticated interpolation during the intensity transformation.

In Fig. 4 we show a second view of the same dotted plane from a slanted pose. In this image, we have been able to cluster also the diagonal points of the grid into a third set of circles. The rewarped image shows the accurate estimate of the pan and the tilt because the back-projected lines are perpendicular. The estimates for the image center from these two views are (353.89,233.38) and (353.697,239.58), respectively. The estimates of the scaling factor are 172.16 and 164.282.

In the third experiment we recorded images of the ceiling containing several natural edges which are perpendicular to each other. Although the angle spanned by the landmarks is quite small the rewarped images show an amazing accuracy in the estimates both of the intrinsics and the pan-tilt of the ceiling with respect to the camera.

6. Conclusion

We introduced a novel method of intrinsic parameter estimation for an orthographic camera in front of a paraboloid mirror. We showed that two vanishing points can reveal the entire information about the scale factors, the image center, and the angle to the plane spanned by the two parallel line sets. The vanishing points can be obtained by taking the intersections of circles having collinear centers. We presented an easily reproducible algorithm including all the curve fitting steps. Performance in real experiments was tested by rewarping onto virtual planes parallel to the actual scene planes. This paper not only

fills a gap in the use of a commercial system but also paves the ground for a series of geometric results in catadioptric vision. In the immediate future we are studying the estimation theoretic part of the fitting in order to take into account appropriate noise models.

References

- [1] T. Boulton. Remote reality demonstration. In *IEEE Conf. Computer Vision and Pattern Recognition*, pages 966–967, Santa Barbara, CA, June 23–25, 1998.
- [2] J. Chahl and M. Srinivasan. Range estimation with a panoramic sensor. *Journal Opt. Soc. Am. A*, 14:2144–2152, 1997.
- [3] K. Daniilidis and M. Spetsakis. Understanding noise sensitivity in structure from motion. In Y. Aloimonos, editor, *Visual Navigation*, pages 61–88. Lawrence Erlbaum Associates, Hillsdale, NJ, 1996.
- [4] C. Fermüller and Y. Aloimonos. Ambiguity in structure from motion: Sphere vs. plane. *International Journal of Computer Vision*, 28:137–154, 1998.
- [5] A. Fitzgibbon, M. Pilu, and R. Fisher. Direct least-square fitting of ellipses. In *Proc. Int. Conf. on Pattern Recognition*, pages 253–257, Vienna, Austria, Aug. 25–30, 1996.
- [6] J. Gluckman and S. Nayar. Ego-motion and omnidirectional cameras. In *Proc. Int. Conf. on Computer Vision*, pages 999–1005, Bombay, India, Jan. 3–5, 1998.
- [7] A. Hicks and R. Bajcsy. Reflective surfaces as computational sensors. In *CVPR-Workshop on Perception for Mobile Agents, Fort Collins, CO, June 26, 1999*.
- [8] S. Maybank. Algorithm for analyzing optical flow based on the least squares method. *Image and Vision Computing*, 4:38–42, 1986.
- [9] V. Nalwa. Bell labs 360-degree panoramic webcam. News Release, <http://www.lucent.com/press/0998/980901.bla.html>, 1998.
- [10] S. Nayar. Catadioptric omnidirectional camera. In *IEEE Conf. Computer Vision and Pattern Recognition*, pages 482–488, Puerto Rico, June 17–19, 1997.
- [11] Y. Onoe, K. Yamazawa, H. Takemura, and N. Yokoya. Telepresence by real-time view-dependent image generation from omnidirectional video streams. *Computer Vision and Image Understanding*, 71:588–592, 1998.
- [12] D. W. Rees. Panoramic television viewing system. United States Patent No. 3, 505, 465, Apr. 1970.
- [13] D. Southwell, A. Basu, and B. Vandergrind. A conical mirror pipeline inspection system. In *Proc. IEEE Int. Conf. on Robotics and Automation*, pages 3253–3258, 1996.
- [14] T. Svoboda, T. Padjla, and V. Hlavac. Epipolar geometry for panoramic cameras. In *Proc. 6th European Conference on Computer Vision*, pages 218–231, 1998.
- [15] E. Trucco and A. Verri. *Introductory Techniques for 3-D Computer Vision*. Prentice Hall, Upper Saddle River, NJ, 1998.
- [16] Y. Yagi, S. Kawato, and S. Tsuji. Real-time omnidirectional image sensor (copis) for vision-guided navigation. *Trans. on Robotics and Automation*, 10:11–22, 1994.

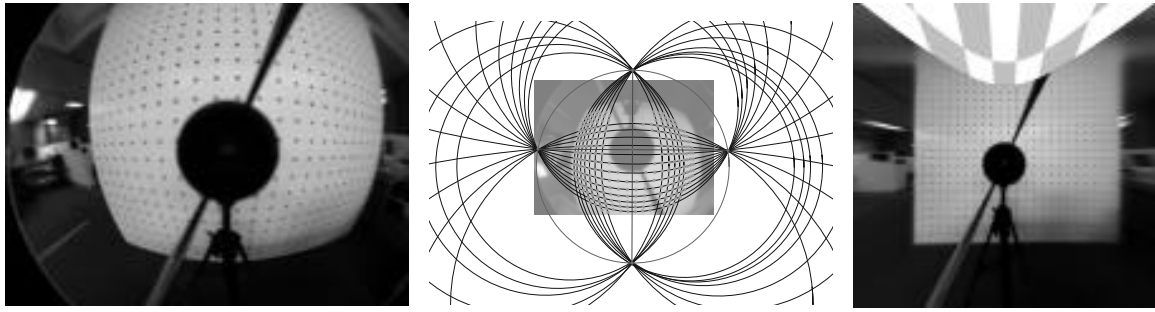


Figure 3: Left: Original image of the dotted plane recorded by the catadioptric camera in frontoparallel pose. Middle: Two groups of circles fitted on the horizontal and vertical dot lines, respectively. The lines through the vanishing points intersect at the image center and all the vanishing points lie on a circle. Right: The rewarped image obtained using both the intrinsic parameters as well as the pan-tilt estimate of the plane. The collinearity of the points shows the quality of the intrinsic calibration. The warped checkerboard pattern indicates the missing regions of the original image.

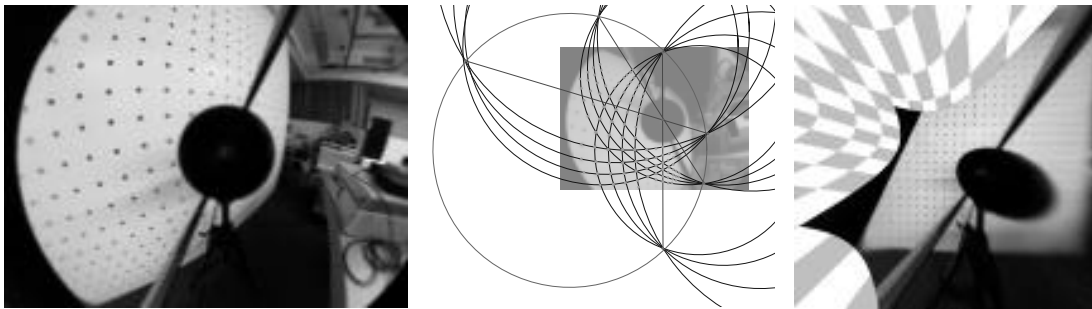


Figure 4: Left: Original image of the dotted plane recorded by the catadioptric camera in slanted pose. Middle: The lines through the three pairs of vanishing points intersect at the image center and all the six vanishing points lie on a circle. Right: The rewarped image obtained using both the intrinsic parameters as well as the pan-tilt estimate of the plane. The collinearity of the points shows the quality of the intrinsic calibration. The perpendicularity of the dotted pattern shows the accurate estimate of the plane normal.

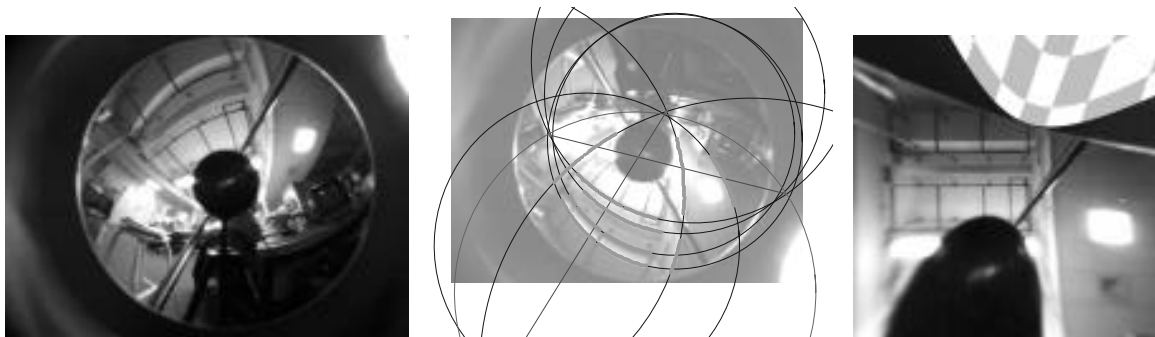


Figure 5: Left: Original image of the ceiling recorded by the catadioptric camera slanted approx. 45 deg. with respect to the ceiling. Middle: Two groups of four and three circles, respectively, fitted on the images of the ceiling-edges. The lines through the vanishing points intersect at the image center and all the vanishing points lie on a circle. Right: Both, the collinearity of the edge elements and the perpendicularity of the edges show a superior performance in estimating intrinsics as well as pan-tilt of the ceiling using only natural landmarks.